Journal of Alloys and Compounds 504S (2010) S275–S278

Contents lists available at ScienceDirect

Journal of Alloys and Compounds

journal homepage: www.elsevier.com/locate/jallcom

Dissimilar friction welding of tubular Zr-based bulk metallic glasses

Hyung-Seop Shin [a,*], Jung-Soo Park [a], Yoshihiko Yokoyama [b]

[a] School of Mechanical Engineering, Andong National University, Andong, Kyungbuk 760-749, Republic of Korea
[b] Advanced Research Center of Metallic Glasses, Institute for Materials Research, Tohoku University, Sendai 980-8577, Japan

ARTICLE INFO

Article history:
Received 29 June 2009
Received in revised form 9 January 2010
Accepted 10 February 2010
Available online 18 February 2010

Keywords:
Bulk metallic glass
Tubular shape
Dissimilar friction welding
Residual strength

ABSTRACT

In this study, the similar and dissimilar friction welding of tubular Zr-based BMGs to BMGs and crystalline metals have been tried and compared with the cases of BMG rods.

In order to characterize the friction weld interface, the morphology of protrusion formed and the temperature distribution at weld interface during friction welding were measured, and micrographic observation and X-ray diffraction analysis on the weld cross-section were carried out. In the case of friction welding of tubular BMGs, it was possible to suppress the development of protrusion formed at the interior of tube by introducing an insert into the joining part of tube specimen. A successful joining of the bulk metallic glass (BMG) to crystalline metals could be obtained for certain pairs of the material combination through the precise control of friction conditions. The residual strength after friction welding was evaluated by the 4-point bending test and compared with the cases of BMG rods.

1. Introduction

The bulk metallic glasses (BMGs) have been developed for structural applications utilizing their superior mechanical properties. However, the availability of various sizes to be used for engineering and structural application fields is still limited. Also, the geometry of component for applications becomes complicated like tube or cylinder type. Therefore, efforts to solve the size limit problem have been performed through various joining processes like friction welding, pulse-current welding, electron-beam welding and spark welding. There has been reported that some studies had succeeded in joining of similar and dissimilar BMG rods [1–5]. In this study, the similar and dissimilar friction welding of tubular Zr-based BMGs to BMG alloys and crystalline metals (Al-alloy) have been tried and compared with the cases of BMG rods [5,6].

2. Experimental procedures

In this study, 2 kinds of Zr-based BMGs having compositions of $Zr_{50}Cu_{40}Al_{10}$ and $Zr_{41.5}Ti_{13.8}Cu_{12.5}Ni_{10}Be_{22.5}$ (Vit-1) were supplied. The $Zr_{50}Cu_{40}Al_{10}$ was supplied from IMA, Tohoku University with a cylindrical rod shape which was prepared by using a tilt casting technique with two-step arc melting process [7]. On the other hand, the Vit-1 specimen was machined from a commercially available 7 mm thickness plate into a rod of 6 mm diameter. Then the tubular specimens were machined from the rod using a hard metal tool by drilling. Fig. 1 shows dimensions of tubular BMG specimens used for friction welding. The thermal properties of Zr-based BMGs measured using DSC are shown in Table 1. As crystalline materials for dissimilar friction welding of Zr-based BMGs, aluminum alloys of A5083 and A5056 were selected.

Table 1
Thermal properties of BMG specimens supplied for friction welding.

Compositions	T_g (K)	T_x (K)	ΔT_x (K)	Note
$Zr_{50}Cu_{40}Al_{10}$	706	792	86	Eutectic
$Zr_{41.5}Ti_{13.8}Cu_{12.5}Ni_{10}Be_{22.5}$	623	705	82	Vitroley-1

An apparatus devised for the friction welding of BMG rods which adopts a pneumatic actuator and gripper based on a conventional lathe was used. The details of the apparatus and welding procedure were described in previously reported Refs. [5,6]. The friction pressure and time adopted in this study were in the range of 150 MPa and 0.6–0.8 s, respectively. During friction welding, the temperature distribution around the weld interface of specimens was measured using an infrared imager (FLIR-ThermaCam SC-2000). After the welding test, the shape and volume of the protrusion formed were examined. The volume of protrusion produced can be derived by measuring the difference in specimen length before and after welding and multiplying the original cross-sectional area to it. In order to characterize the friction weld interface of BMGs, X-ray diffraction analysis (XRD) and micrographic observation were also carried out on the cross-section of weld specimens. Finally, the residual strength at fracture point of weld specimens was evaluated by using a four-bending test [6].

3. Experimental results and discussion

In the case of friction welding of tubular specimens, the protrusions were formed both at the inner and outer surfaces of weld interface. The formation of protrusion at the inner surface could be reduced to the minimum level by introducing an insert core into joining part of tubular specimens.

* Corresponding author at: School of Mechanical Engineering, Andong National University, #388 Songchun-dong, Andong, Kyungbuk 760-749, Republic of Korea. Tel.: +82 54 820 5675; fax: +82 54 820 5167.
E-mail address: hsshin@andong.ac.kr (H.-S. Shin).

0925-8388/$ – see front matter
doi:10.1016/j.jallcom.2010.02.047

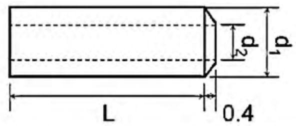

Diameter	d_1 (mm)	d_2 (mm)	L(mm)	Note
5 mm	5.0	3.0	24	$Zr_{50}Cu_{40}Al_{10}$
6 mm	6.0	4.0	27	Vit-1

Fig. 1. Dimensions of tubular BMG specimens for friction welding.

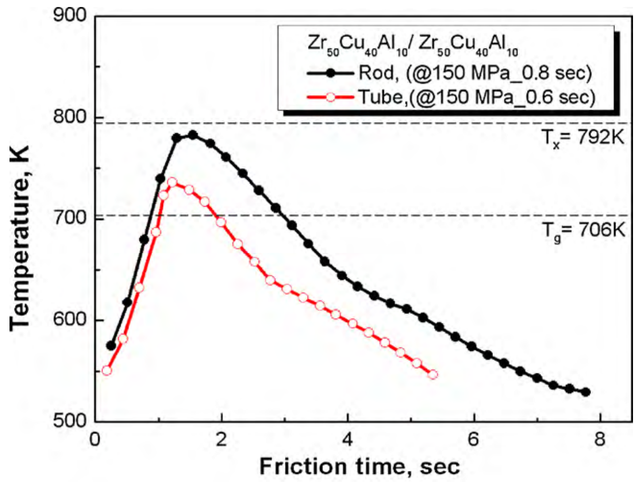

Material combination	Specimen geometry	Protrusion volume (mm^3)	Maximum temperature (K)
$Zr_{50}Cu_{40}Al_{10}$ /$Zr_{50}Cu_{40}Al_{10}$	Solid	68.9	787
	Tube	55.0	733

Fig. 2. Effect of specimen geometry on weld interface temperature and protrusion volume formed during similar friction welding of $Zr_{50}Cu_{40}Al_{10}$ BMG.

The friction welding of tubular Zr–Cu–Al BMGs was conducted at the same weld conditions of friction pressure (P_f = 150 MPa) and friction time (t_f = 0.8 s) as the cases of BMG rods [6]. During friction welding of the $Zr_{50}Cu_{40}Al_{10}$ BMG, the temperature distributions around the weld interface of specimens and the volume of protrusion formed were measured and shown in Fig. 2. There existed the effect of specimen geometry. The tubular BMG specimens showed a reduced maximum temperature on weld interface as compared with the cases of BMG rods. It was resulted from a higher thermal conduction in the case of tubular specimen. Then the volume of protrusion was also smaller than the case of BMG rod due to less cross-sectional area in the tubular specimen.

Based on the similar friction welding of tubular BMG and our previous results on the dissimilar friction welding of BMGs to crystalline metals [5,6], the dissimilar friction welding of the tubular Zr-based BMGs to crystalline metals of A5056 and A5083 alloy were carried out. Fig. 3 shows appearances after dissimilar friction welding of tubular BMGs to Al-alloys. In the cases of Vit-1/A5056 and

Material Combination	Weld condition	Appearance
Vit-1/A5056	150 MPa_0.6 sec	 3 mm
Vit-1/A5083		 3 mm
$Zr_{50}Cu_{40}Al_{10}$/ A5083		 3 mm

Fig. 3. Appearances after dissimilar friction welding of tubular BMGs to Al-alloy.

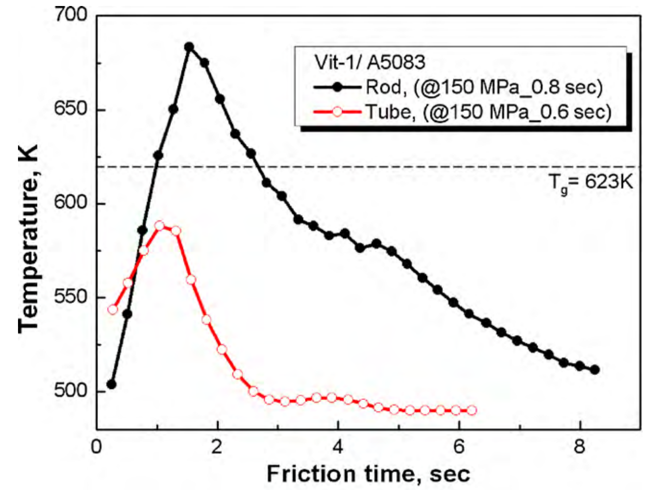

Material combination	Specimen geometry	Protrusion Volume (mm^3)
Vit-1 /A5083	Solid	102.0
	Tube	15.7

Fig. 4. Effect of specimen geometry on weld interface temperature and protrusion volume during dissimilar friction welding of Vit-1 BMG/A5083 combination.

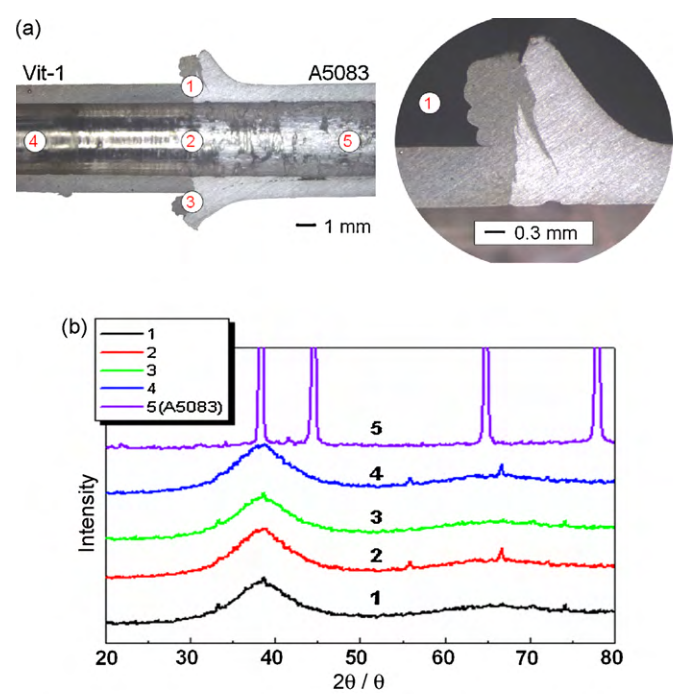

Fig. 5. (a) Cross-sectional view and (b) X-ray diffraction patterns around the interface after dissimilar friction welding of tubular Vit-1 BMG to A5083.

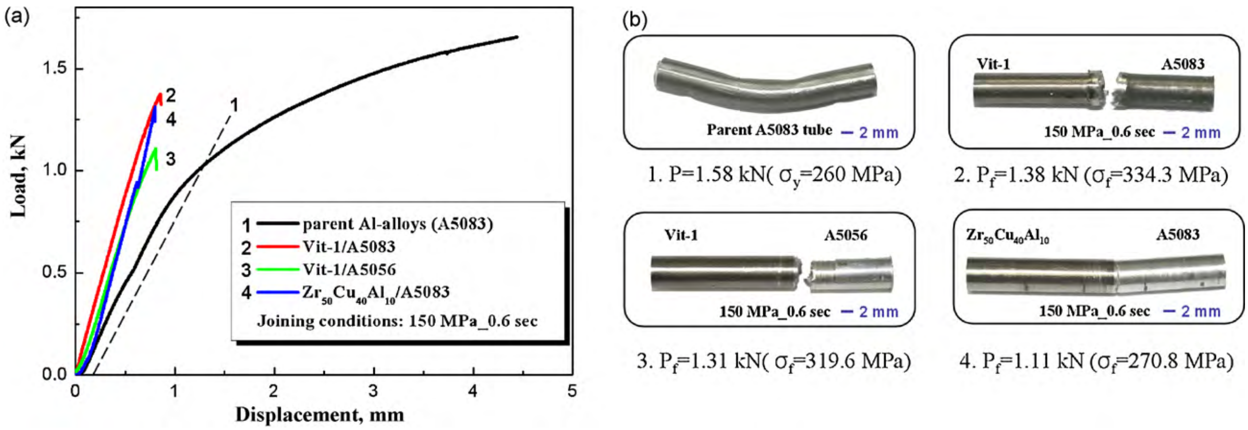

Fig. 6. (a) Load–displacement curves for BMG/Al-alloys combination by 4-point bending test and (b) appearances after fracture.

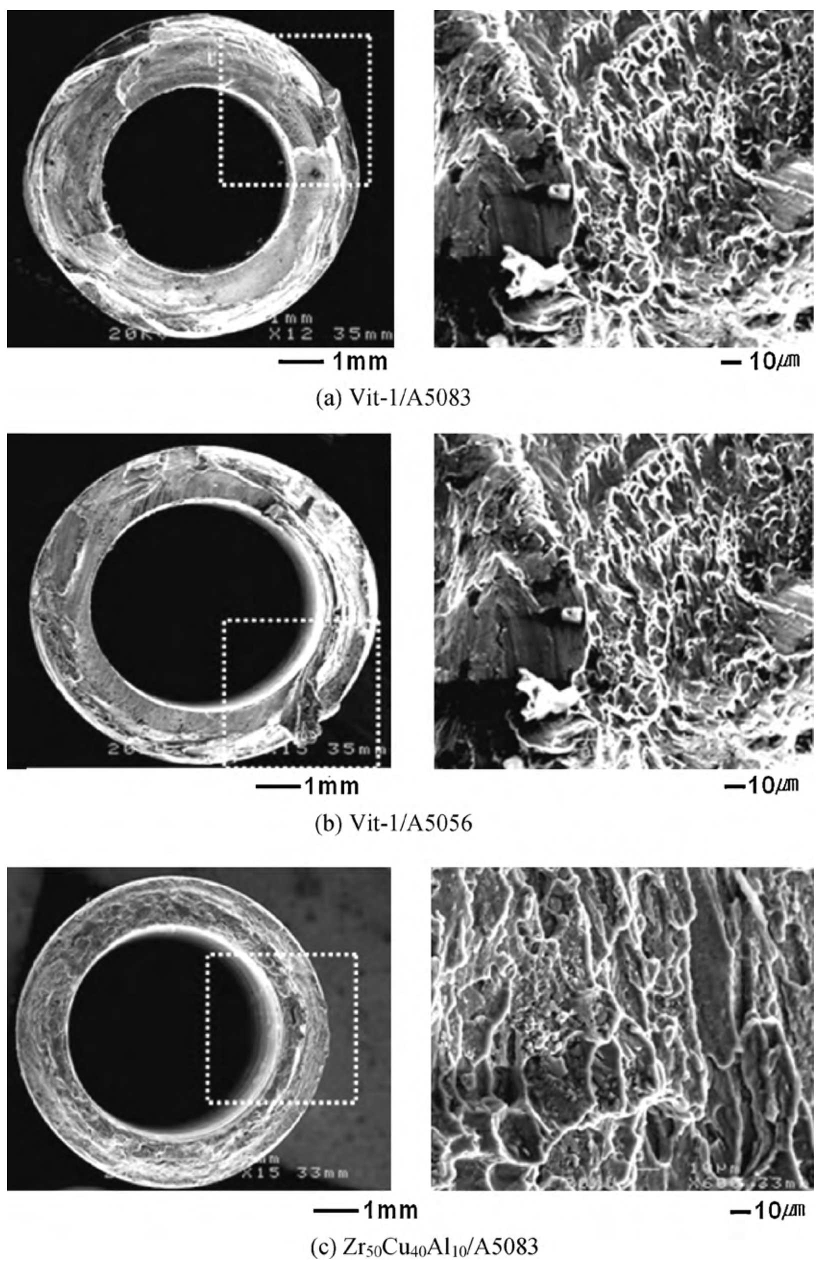

Fig. 7. SEM fractographic images at BMG side after 4-point bending test for dissimilar friction weld BMG/Al-alloy combinations.

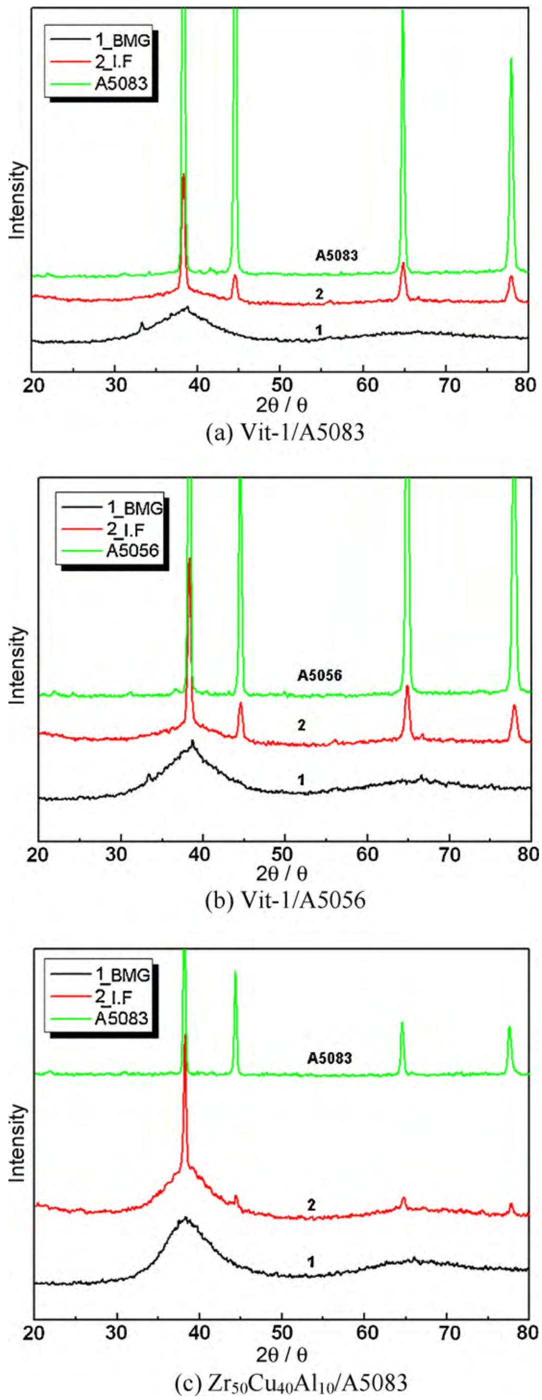

Fig. 8. X-ray diffraction patterns at fracture surfaces for dissimilar friction weld BMG/Al-alloy combinations shown in Fig. 7.

$Zr_{50}Cu_{40}Al_{10}$/A5083 combinations, the protrusion was only formed from the Al-alloy side, but not formed from the BMG side. The case of Vit-1/A5083 combination represented a well-developed protrusion from both sides.

For the Vit-1/A5083 combination, therefore, variation of maximum temperature on the weld interface and volume of protrusion during friction welding were investigated and shown in Fig. 4. Similarly to the case of similar friction welding shown in Fig. 2, the dissimilar friction welding of tubular BMG specimen to crystalline materials also showed the similar results of lower temperature and less protrusion volume as compared with cases of rods.

Fig. 5(a) shows optical micrographs of polished cross-section for the dissimilar friction weld Vit-1/A5083 combination. No visible defects or voids can be seen at the weld interface and the protrusion was generated from both sides of specimens. Fig. 5(b) shows micro-XRD patterns at each part of the cross-section, interface, protrusion and base metal part, respectively. All BMG parts remained as an amorphous phase after friction welding. Also, the diffraction pattern of crystalline phase of A5083 was plotted. From the cross-section and XRD pattern observations, it can be thought that there occurred a good metallurgical joining between tubular BMG and A5083 materials without any crystallization at around the interface of the BMG part.

In order to evaluate the residual strength at the weld part after dissimilar friction welding of tubular Zr-based BMG to crystalline metals, a 4-point bending test was carried out. In all cases, the fracture occurred at the weld interface, as shown in Fig. 6(a), but the residual bending strength calculated by the fracture load, σ_f, represented a higher value than the yield strength of A5083 alloy as shown in Fig. 6(b).

These high residual strengths for the dissimilar friction welding of the Zr-based BMGs/Al-alloy combinations were resulted from good metallurgical joining, which could be seen by typical ductile fracture appearances including the dimples observed on the fracture surfaces as shown in Fig. 7.

Fig. 8 shows micro-XRD patterns at weld interface on the fracture surface of the BMG side of Zr-based BMG/Al-alloy combination. The XRD pattern represents that the amorphous phase existed at the BMG side. And the diffraction peak of crystalline phase of Al-alloy at the weld interface of BMG side (marked as 2_I.F) represents the occurrence of metallurgical joining during the dissimilar friction welding of BMGs to crystalline Al-alloys.

4. Summary

(1) The similar friction welding of BMG tubes was successfully achieved at the same weld condition as the cases of BMG rod. In that case, the protrusion formed at the inner surface of tube could be suppressed by introducing an insert into joining part of tube specimen.
(2) Both the volume of protrusion formed and the temperature measured during similar and dissimilar friction welding of tubular BMG specimens were less than the case of BMG rods.
(3) In the case of dissimilar friction welding of tubular Vit-1 BMG/A5083 combination, a good metallurgical joining at weld interface could be achieved. Therefore it represented a high residual strength exceeding the yield strength of A5083 without the occurrence of crystallization at the weld interface.

Acknowledgements

This works was supported by Korea Research Foundation Grant funded by the Korean Government (MOEHRD) (KRF-2006-041-D00280 and KRF-2007-511-D00003).

References

[1] For example Y. Kawamura, Mater. Sci. Eng. A 375–377 (2004) 112–119.
[2] Y. Kawamura, Y. Ohno, Scripta Mater. 45 (2003) 127–137.
[3] T. Shoji, Y. Kawamura, Y. Ohno, Mater. Trans. 44 (2003) 1809–1816.
[4] H.S. Shin, Y.J. Jeong, H.Y. Choi, H. Kato, A. Inoue, Mater. Trans. 46 (2005) 2768–2772.
[5] H.S. Shin, Y.J. Jeong, H.Y. Choi, H. Kato, A. Inoue, J. Alloys Compd. 434–435 (2007) 102–105.
[6] H.S. Shin, J.S. Park, Y.C. Jung, J.H. Ahn, Y. Yokoyama, A. Inoue, J. Alloys Compd. 483 (2009) 182–185.
[7] Y. Yokoyama, K. Inoue, K. Fukaura, Mater. Trans. 43 (2002) 2316–2319.